J Mater Sci: Mater Med (2011) 22:693–704
DOI 10.1007/s10856-011-4248-0

Fabrication and cell affinity of biomimetic structured PLGA/articular cartilage ECM composite scaffold

Xifu Zheng · Fei Yang · Shenguo Wang · Shibi Lu · Weiguo Zhang · Shuyun Liu · Jingxiang Huang · Aiyuan Wang · Baosheng Yin · Ning Ma · Li Zhang · Wenjing Xu · Quanyi Guo

Received: 25 September 2010 / Accepted: 22 January 2011 / Published online: 3 February 2011

Abstract An ideal scaffold for cartilage tissue engineering should be biomimetic in not only mechanical property and biochemical composition, but also the morphological structure. In this research, we fabricated a composite scaffold with oriented structure to mimic cartilage physiological morphology, where natural nanofibrous articular cartilage extracellular matrix (ACECM) was used to mimic the biochemical composition, and synthetic PLGA was used to enhance the mechanical strength of ACECM. The composite scaffold has well oriented structure and more than 89% of porosity as well as about 107 μm of average pore diameter. The composite scaffold was compared with ACECM and PLGA scaffolds. Cell proliferation test showed that the number of MSCs in ACECM and composite scaffolds was noticeably bigger than that in PLGA scaffold, which was coincident with results of SEM observation and cell viability staining. The water absorption of ACECM and composite scaffolds were 22.1 and 10.2 times respectively, which was much higher than that of PLGA scaffolds (3.8 times). The compressive modulus of composite scaffold in hydrous status was 1.03 MPa, which was near 10 times higher than that of hydrous ACECM scaffold. The aforementioned results suggested that the composite scaffold has the potential for application in cartilage tissue engineering.

Xifu Zheng and Fei Yang contribute equally to this manuscript.

X. Zheng · W. Zhang
Department of Orthopedic Surgery, First Affiliated Hospital of Dalian Medical University, Dalian 116011, China

X. Zheng · S. Lu · S. Liu · J. Huang · A. Wang · B. Yin · N. Ma · L. Zhang · W. Xu · Q. Guo (✉)
Institute of Orthopedics of Chinese PLA, Chinese PLA General Hospital, No. 28 Fuxing Road, Haidian District, Beijing 100853, People's Republic of China
e-mail: guoquanyi301@gmail.com

F. Yang · S. Wang
BNLMS, Institute of Chemistry, Chinese Academy of Sciences, Beijing 100080, China

1 Introduction

An ideal tissue engineering scaffold should have the following characteristics: biocompatibility, suitable porosity and pore size, sufficient mechanical strength and good cell affinity [1, 2]. Many porous scaffolds fabricated from various biodegradable materials have been developed and used for tissue engineering. Especially, including naturally derived macromolecules such as collagen [3, 4], hyaluronic acid [5], chitosan [6], fibrin [7] and synthetic polymers such as polyglycolide (PGA), polylactide (PLA) [8], polycaprolactone (PCL) [9] and their co-polymers such as poly(lactide-co-glycolide) (PLGA) [10–12] have received enormously attention and been widely used for tissue engineering.

Polylactide type synthetic polymers have been used widely in tissue engineering with the characteristics of satisfactory biocompatibility, low immunogenicity, good mechanical property, absolute biodegradability and controlled biodegradation rate. However, the surface of PLGA is hydrophobic and low intrinsic bioactive for cells adhesion. Natural extracellular matrix (ECM) has good hydrophilicity and provides a suitable microenvironment and informational signals, which facilitate cell attachment, proliferation and differentiation. As a new method to get native ECM, decellularization technique has been adopted to remove cellular antigens and preserve most of structural and functional proteins that constitute ECM. ECM from

various decellularized tissues, including blood vessels, skin, bladder, and so on have been studied for tissue engineering and regenerative medicine applications [13–15]. Decellularized dermis has been applied in clinical therapy and commercialized. Using an improved method of combining physical and chemical decellularization procedure in our study, the ACECM derived porous scaffold was developed with a freeze drying method. In vitro and in vivo studies demonstrated that the ACECM scaffold reserved main components of cartilage glycosaminoglycans (GAGs) and type II collagen, provided adequate space structure and had good biocompatibility for supporting MSCs attachment, proliferation and differentiation into chondrocytes [16]. So the ACECM is a suitable biomaterial candidate for cartilage tissue engineering.

However, the scaffolds made of natural biomaterials are insufficient in mechanical strength especially in hydrous status. ACECM scaffold is the same with lower tensile and compressive strength. An ideal cartilage scaffold seeded with cells should possess structural integrity to temporarily withstand functional loading in vivo as natural cartilage does [17, 18]. That is, it temporarily deforms upon loading with little structural collapse, but recovers to the original geometry upon unloading. In the case of collapse, a high degree of incomplete recovery or permanent deformation occurs upon loading, such a cartilage scaffold can not protect cells be free of pressure lesion and ensure sufficient nutrition provision and wastes discharge.

The aim of tissue engineering and regenerative medicine is to regain structure and function of original tissue architecture. The biochemical composition and structure–function relationship of the scaffold are critical for optimizing mechanical and biological performance. It is significant that the morphological structure of scaffold is biomimetic to the repaired natural tissue [19, 20]. The organization of articular cartilage collagen network has most notable zonal variations, which principally responsible for tensile and compressive properties of cartilage. The alignment of collagen fibers in deep zone cartilage is oriented vertical to the subchondral bone. So the oriented scaffold with vertical microtubules structure would be closely related to physiological and biomechanical function of cartilage.

The composite scaffolds derived naturally and synthetic biomaterials with good cell affinity and enough mechanical strength to serve as an initial support have widely applied in cartilage tissue engineering [21–23]. Despite various scaffolds have been developed, it is remaining significant challenge in fabrication functional and biomimetic scaffold. Although synthetic and naturally derived polymeric materials have their own advantages and drawbacks, the effects of these advantages and drawbacks on properties of the nanofibrous ACECM/PLGA composite scaffold could be respectively enhanced and reduced. So the new biomimetic oriented composite scaffold would be a selectable candidate for cartilage tissue engineering.

2 Materials and methods

2.1 Materials

2.1.1 Synthesis of PLGA (70/30)

L-lactide and glycolide were purchased from PURAC (the Netherlands) and purified by twice recrystallization in dried ethyl acetate (Beijing Tonghua Fine Chemicals Company, China). PLGA (70/30, mol/mol) was synthesized by ring-opening polymerization of lactide and glycolide under 65 Pa in a sealed glass ampoules at 180°C for 20 h in the presence of stannous octoate (0.05 wt%, Sigma, Germany) as catalyst [24]. The raw PLGA (70/30) was purified by dissolving in chloroform and reprecipitating from ethanol, and then followed by drying in vacuum at room temperature for 2 days. The molecular weight of PLGA (70/30) (Mw = 115,000) was determined by Waters510 gel-permeation chromatography (GPC) equipped with Shodex KF-800 columns at 35°C using chloroform as eluent at a flow rate of 1.0 ml/min. The 1,4-dioxane, chloroform and other reagents were of analytical quality and directly used without further treatment.

2.1.2 Pulverization and decellularization of articular cartilage

An improved method for decellularization was adopted and developed according to correlated research [16]. Porcine knee joints were got from abattoir after slaughter immediately, covered with ice bag and transported to laboratory. Cartilage slices were cut from femoral condyle under aseptic conditions. The method to shatter and decellularize with combining physical and chemical procedure was illustrated as follows. The slices were suspended and rinsed in sterile PBS solution three times, then homogenized under powerfully shearing force using a tissue disintegrator to form suspension slurry and centrifugated by differential centrifugation method. The suspension was centrifugated in a centrifuge (Beckman Allegra X-22R, USA) for 5 min at 1,500 rpm with F0850 rotor. The suspended microparticles were separated with precipitated macroparticles. The suspended microparticles were centrifugated for another 5 min at 3,000 rpm and 20 min at 6,000 rpm successively. The cartilage suspended microparticles at 6,000 rpm were centrifugated for 35 min at 9,500 rpm and collected ACECM fibrous precipitation. The precipitation was rinsed and centrifugated twice under 9,500 rpm with sterile PBS solution. The ACECM precipitation was digested in 3%

TritonX-100 and 0.25% trypsin (containing 0.1% EDTA, 0.1% sodium azide) successively with gentle agitation for decellularization 12 h at 4°C, then 12 h in 50 U/ml deoxyribonuclease I and 1 U/ml ribonuclease A (both Sigma) with agitation at 37°C for removing nuclear materials after being washed in PBS without protease inhibition. After decellularization, the ACECM precipitation was centrifugated under 9,500 rpm again. All the nanofibrous ACECM precipitations were preserved in sterile glassware for fabrication scaffolds.

2.2 Scaffolds fabrications

2.2.1 Fabrication of ACECM oriented scaffold

The preserved nanofibrous ACECM was washed twice with sterile PBS and made into predetermined concentration 5% (w/w) suspension. The procedure of fabrication oriented scaffold could be illustrated briefly as follows. After ACECM being infused into a 4 or 8 mm cylindrical mould, the mould was put vertically onto metal plate in a refrigerator maintaining −20°C and frozen for half hour. After frozen completely, the mould was put into refrigerator maintaining −20°C for another 2 h. The mould was then transferred into a freezer dryer and lyophilized for 48 h under vacuum. The ACECM scaffolds were taken out of mould and performed cross-linking by ultraviolet at 258 nm for 4 h. The scaffolds were immersed into 95% (v/v) alcohol solution (containing 50 mM 1-ethyl-3-(3-dimethylaminopropyl) carbodiimide hydrochloride [EDAC] and 20 mM N-hydroxysucinimide [NHS]; Sigma) for 24 h at 4°C. Excess EDAC was rinsed from the scaffolds by using of PBS repeatedly. ACECM oriented scaffolds of approximately 4 or 8 mm in diameter were fabricated.

2.2.2 Fabrication of PLGA oriented scaffold

The PLGA (70/30) was dissolved in dioxane to form a solution with concentration 7% (w/w). The polymer solution was cast into a mold to process the phase separation guided by temperature gradient. The super cooling temperature was controlled at −20°C [25]. After the phase separation, the solid solution was taken out and freeze-dried under vacuum (less than 45 Pa) for 72 h. Finally, the produced microtubules oriented scaffold was further dried under vacuum at room temperature for 48 h to remove the residual solvent and preserved in a 4°C refrigerator for use.

2.2.3 Fabrication of PLGA/ACECM composite oriented scaffold

PLGA was dissolved in dioxane to form a solution with a concentration of 10%. ACECM was added into solution with the same weight of PLGA to form slurry. Then the concentration was adjusted to 7% (w/w) by add some dioxane. Then the slurry was cast into a mold. The same phase separation technique above to fabricate oriented PLGA scaffold was processed. Then the solid slurry was taken out and freeze-dried under vacuum for more than 72 h. The produced oriented scaffold was washed by water to remove residual dioxane. Then scaffolds were freeze-dried and preserved in a 4°C refrigerator for use.

2.3 Evaluation of nanofibrous ACECM and oriented scaffold

2.3.1 Microstructure of nanofibrous ACECM

To observe the morphology and diameter of nanofibrous ACECM, the ACECM precipitations were made into 3% (w/w) suspension and smeared onto microscopic slide. Then the ACECM was dehydrated through a series of graded alcohols and dried at room temperature, the samples were sputter-coated with gold and observed by scanning electron microscope (SEM), (BCPCAS-4800 Hitachi Japan).

2.3.2 Histology and immunohistochemistry assay of ACECM oriented scaffold

ACECM scaffolds were mounted by using of O.C.T. compound (Tissue-Tek, Miles, USA). Cryosections (10 μm thick) were cut and fixed in acetone for 30 min at room temperature, slightly washed with PBS. The samples were observed by toluidine blue and safranin O stainings for identification the presence of cartilage derived GAGs.

The type II collagen was stained immunohistologically using porcine anti-collagen-II polyclonal antibody according to instruction. In brief, cross and vertical sections were blocked with peroxidase blocking solution for 10 min and then 10% (v/v) goat serum solution for 30 min. The sections were then incubated with anti-type II collagen (1:100 working dilution) overnight at 4°C. The biotinylated secondary antibody (anti-rabbit FITC-conjugated immunoglobulins; Shiankexing, Beijing) was applied for 30 min followed by incubation with horseradish peroxide-conjugated streptavidin for 10 min. Color was developed with diaminobenzidine tetrahydrochloride (DAB). Images were examined by microscopy and photograph.

2.4 Characterization of the oriented scaffolds

After scaffolds were coated with gold using a sputter coater (Desk-II; Denton Vacuum Inc.), morphology of scaffolds was observed by SEM (JSM-6700F; JEOL, Tokyo, Japan). Diameter of microtubules of oriented scaffold was calculated according to SEM micrographs. For each scaffold,

average pore diameter of the microtubules was calculated according to determined diameter of 100 microtubules which in a magnification ×100 of SEM micrograph.

The porosity of oriented scaffolds was determined according to a reported method [26], where a density bottle was used to instead of a graduated cylinder. Firstly all samples were cut into quadrate pieces with near 0.5 cm of height (H), length (L) and width (W). Then all the sizes of pieces were carefully measured by a vernier caliper, and the volumes (Vw) of scaffolds including volume of scaffold pore and volume of scaffold skeleton were calculated. At 30°C the density bottle was filled with ethanol (density ρe) and weighed ($W1$). Scaffold sample (weight Ws) was immersed into density bottle and kept at 30°C again for 30 min. All overflowed ethanol was cleaned away carefully. Then the density bottle was weighed again ($W2$). The parameters of scaffolds including volume of whole scaffold (Vp), volume of scaffold skeleton (Vs) and porosity (ε) of scaffold were calculated as follows:

$$Vw = H \times L \times W \tag{1}$$

$$V\mathrm{s} = (W1 - W2 + W\mathrm{s})/\rho\mathrm{e} \tag{2}$$

$$\varepsilon = 1 - V\mathrm{s}/V\mathrm{p} \tag{3}$$

2.5 Mechanical analysis of oriented scaffolds

According to reported methods, the mechanical properties of three types of oriented scaffolds in both dry and hydrous status were determined respectively by measuring compressive modulus [22]. Before test, the scaffold samples were processed by a razor blade to rectangle fit in a test chamber of the mechanical analyzer (MTS Tytron 250 USA). The stress–strain curve was generated from a chart recorder by applying a constant compressive strain at a crosshead speed of 1 mm/min. The compressive modulus was calculated using following formula:

$$E = \Delta P/A \times L/\Delta L \tag{4}$$

where E is compressive modulus (modulus of elasticity, MPa); ΔP is compressive force margin of the two points on linear segment of curve before the first break point; ΔL is displacement margin of the corresponding two points changes; A is area through which the force is applied; L is original thickness of tested scaffold. Scaffolds were dipped in PBS (pH 7.4) for 2 h at 25°C before testing mechanical strength in hydrous status.

2.6 Water absorption ratio

Water absorption property of the three types of oriented scaffolds (n = 3/group) was assessed as follows. The completely dried scaffolds were weighted (Wdry) and then dipped in deionised water for water absorption equilibration at room temperature for 4 h. Then the hydrous scaffolds were removed from water and removed the surface free water by filter paper. Final the hydrous scaffolds were weighted (Wwet) and water absorption was calculated with the formula:

$$\text{Water absorption ratio } (\%) = (\mathrm{Wwet} - \mathrm{Wdry})/\mathrm{Wdry} \times 100 \tag{5}$$

2.7 Cell culture

With approval from the local Animal Care Committee of Chinese PLA general hospital, mature New Zealand White rabbits (weight 2.5–3.0 kg) were anaesthetized. Mesenchymal stem cells (MSCs) isolation and culture were performed as previously described [27]. In brief, bone marrow samples were obtained from 8 ml of aspirates of iliac crest, then layered over a lymphoprep gradient and centrifuged at 2,000 rpm for 20 min at room temperature. Mononuclear cells were separated and washed twice with Hank's solution. Cells were resuspended in regular growth medium containing low glucose content Dulbecco's modified Eagle's medium (DMEM-LG, Sigma, USA) supplemented with 15% FBS and seeded at a concentration of 1×10^6 cells/cm^2. Cells were cultured in a humidified atmosphere with 5% CO_2 at 37°C. The medium was changed every other day until cells became 90% confluence. The cells were digested with 0.25% trypsin solution and seeded with a density of 1×10^4 cells/cm^2 in regular growth medium for expansion. The P3 cells were used in the experiment.

2.8 Cell seeding and morphology observation

The MSCs were resuspended in culture medium. The oriented scaffolds (4 mm diameter, 1 mm thickness) were sterilized by ethylene oxide and placed into a 24-well culture plate and 20 μl cell suspensions with approximately 1×10^5 cells was seeded onto each sample until the scaffold became completely saturated. The scaffolds were cultured under a 5% CO_2 humidified atmosphere at 37°C 4 h for cell adherence, and then 2 ml of culture medium was added to each well. After cells were cultured on scaffolds for 3 days, the samples were washed with PBS and fixed with 2.5% glutaraldehyde for 24 h at 4°C. Then the scaffolds were dehydrated through a series of graded alcohols and dried at room temperature, the samples were sputter-coated with gold. Finally, the morphology of adhered cells in scaffold was observed by SEM.

2.9 Cell proliferation assay

Cell proliferation was evaluated quantitatively by cell counting kit-8 (CCK-8 kit, Dojindo Laboratories Japan) to

cell count, which is a colorimetric method for determining the number of viable cells in culture. Three types of oriented scaffolds were placed into a 24-well culture plate and 15 μl cell suspensions with approximately 5×10^4 cells was seeded onto the top surface of scaffold (4 mm diameter, 1 mm thickness) and allowed to penetrate into scaffold. The cells/scaffold structures were then incubated at 37°C under 5% CO_2 condition 4 h for cell adherence. After cell adherence, the structures were transferred to a new 24-well plate and cultured in medium for an additional 1, 3 and 7 day. At every indicated time interval, culture medium was discarded and approximately 500 μl serum-free DMEM medium with 50 μl CCK-8 solution were added to each sample successively, followed by incubation at 37°C for 3 h to formazan product. Supernatant was transferred to 96-well plate, the optical density (OD) at 450 nm was determined using a microplate reader (Beckman, Fullerton, CA), which represented the number of viable cells in the scaffolds.

2.10 Cell viability assay

Cell viability in cells/scaffold structures was evaluated at 3 and 7 days using a Live/Dead assay kit (FDA-PI, Sigma) according to instruction. Media was aspirated from cultures and the structures were washed in PBS then incubated in a 5×10^{-3} mg/ml FDA working solution for 5 min at 37°C under dark conditions. The fluorescent dye was aspirated and structures were washed twice in PBS. The structures were incubated in a 5×10^{-3} mg/ml PI working solution for another 5 min. After which the PI solution was aspirated and the structures were washed twice with PBS before being viewed by an Olympus IX81 confocal microscope (Olympus, Japan).

2.11 Statistical analysis

All quantitative data were analyzed and expressed as the mean ± standard deviation. CCK-8 evaluation, water uptake evaluation and compressive modulus results were assessed by one way analysis of variance (ANOVA). The comparison between two means was analyzed using Tukey's test, which $P < 0.05$ was considered statistical significance.

3 Results

3.1 Characterization and biochemical composition of ACECM

The morphology and diameter of ACECM fibers were observed by SEM in Fig. 1a, c. The decellularized ACECM was fibrous shape and nanometer size. Comparing with standard scale, it could be seen that the diameter of nanofibrous ACECM was about 50 nm uniformly. The nanofibrous and orientation structured characteristics of ACECM scaffold were displayed in Fig. 1b, d. In cross section of ACECM scaffold, the nanofibrous ACECM interconnected and aligned randomly (Fig. 1b); some of the nanofibers were connected during the pore space. Figure 1d showed that the nanofibrous ACECM aligned along vertical orientation in the vertical section. For evaluating the biochemical

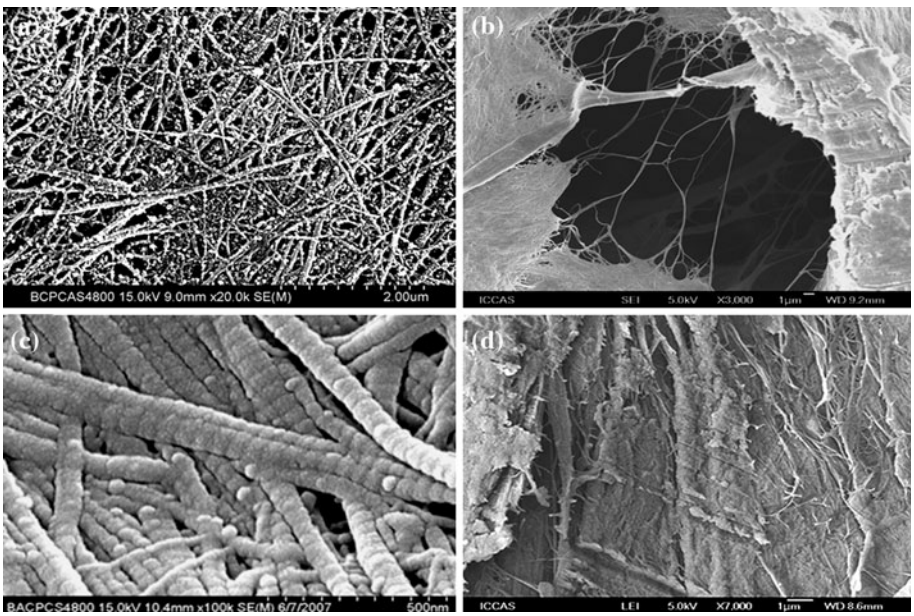

Fig. 1 SEM micrographs: morphology, diameter of ACECM and the wall of oriented ACECM scaffold. Morphology and diameter of nanofibrous ACECM (**a**, **c**); the morphology and nanofibrous ECM orientation of ACECM scaffold wall (**b**, **d**)

composition of oriented ACECM scaffold, histological and immunofluorescent stainings were carried out. Immunofluorescent staining revealed the presence of collagen II, while positive stainings of toluidine blue and safranin O indicated that GAGs were existed in oriented scaffold (Fig. 2). The vertical sections of ACECM scaffold indicated the oriented structure.

3.2 Characterization of oriented scaffolds

Microstructure of oriented PLGA, ACECM and composite scaffolds was observed by SEM as shown in Fig. 3. The SEM graphs (Fig. 3a, b and c) showed the cross section of these oriented scaffolds. It could be seen that all the scaffolds possessed interconnected porous structure and the pore distributed uniformly. Others SEM graphs demonstrated the structural feature of vertical orientation. The vertical microtubules interconnected and aligned congruously. The morphological characteristics of the composite scaffold (Fig. 3a, d and g) were similar to the PLGA (Fig. 3b, e and h) and ACECM (Fig. 3c, f and i) scaffolds, except there were some micropores in the wall of oriented microtubules and the surface appeared to be rough. Porosity and pore diameter were illustrated as follows. The porosities of three kinds of oriented scaffolds were very high as expectation. The porosity of PLGA was 90 ± 2%; while the ACECM was 93 ± 3%. The porosity of composite oriented scaffold was 89 ± 2%. The average pore diameter of the composite scaffold was 107 μm. The pore diameter was 104 and 105 μm for the PLGA and ACECM scaffolds, respectively.

3.3 Water uptake property

After being saturated in aqueous solution, the weights of all three types of oriented scaffolds were greatly increased comparing with the dry scaffolds, especially ACECM and composite groups as shown in Fig. 4. The wet weights of the scaffolds, which indicated hydrophilicity, were higher for the ACECM and composite scaffolds than they were for PLGA scaffolds. The ratios of water weight to dry weight of scaffold were 22.1 ± 0.1 and 10.2 ± 0.2 for the ACECM and composite scaffolds respectively, meanwhile only 3.8 ± 0.3 for the PLGA scaffold.

3.4 Mechanical property of scaffolds

Figure 5 showed the mechanical properties of these oriented scaffolds. In dry status, the compressive modulus of PLGA and ACECM scaffold were 9.3 ± 0.5, 2.20 ± 0.17 MPa respectively; while the composite scaffold was 4.20 ± 0.17 MPa, which was bigger than ACECM scaffold. In the hydrous status, the compressive modulus of ACECM scaffold was only 0.11 ± 0.01 MPa. However, the hydrous composite and PLGA scaffolds displayed more strong mechanical property. The compressive modulus was 1.03 ± 0.1 and 3.53 ± 0.25 MPa respectively.

3.5 Cell morphology and affinity adhered on oriented scaffolds

Figure 6 displayed the morphological characteristics of MSCs adhered on three types of oriented scaffolds after

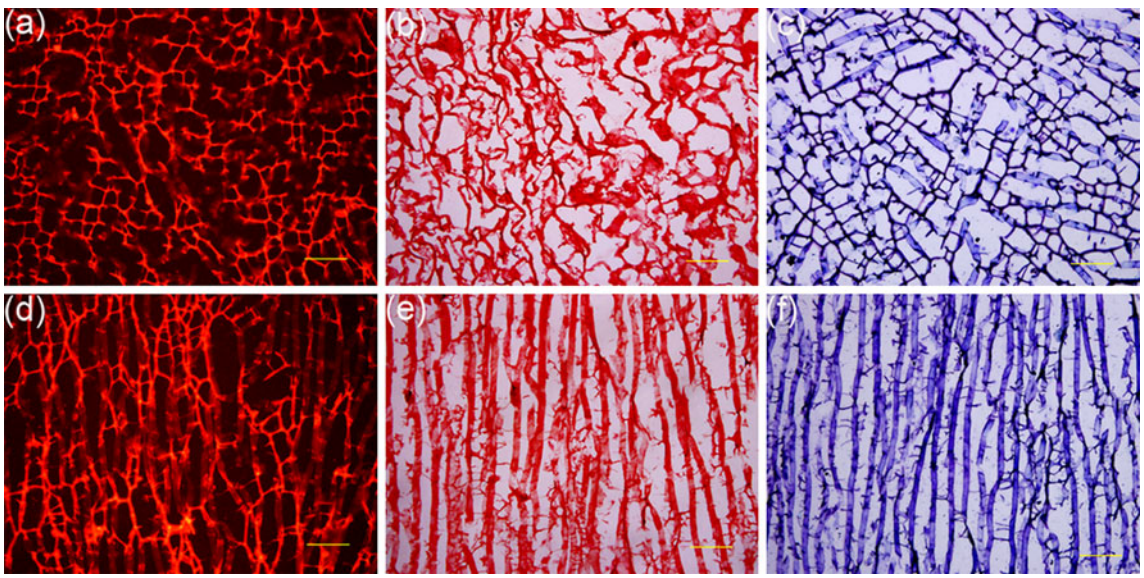

Fig. 2 Collagen II immunohistochemical staining (**a**, **d**), Safranin O (**b**, **e**) and Toluidine blue (**c**, **f**) stains for oriented ACECM scaffold. Fig **a**, **b**, **c** and **d**, **e**, **f** display cross and vertical section of ACECM oriented scaffold respectively. *Bar* = 200 μm

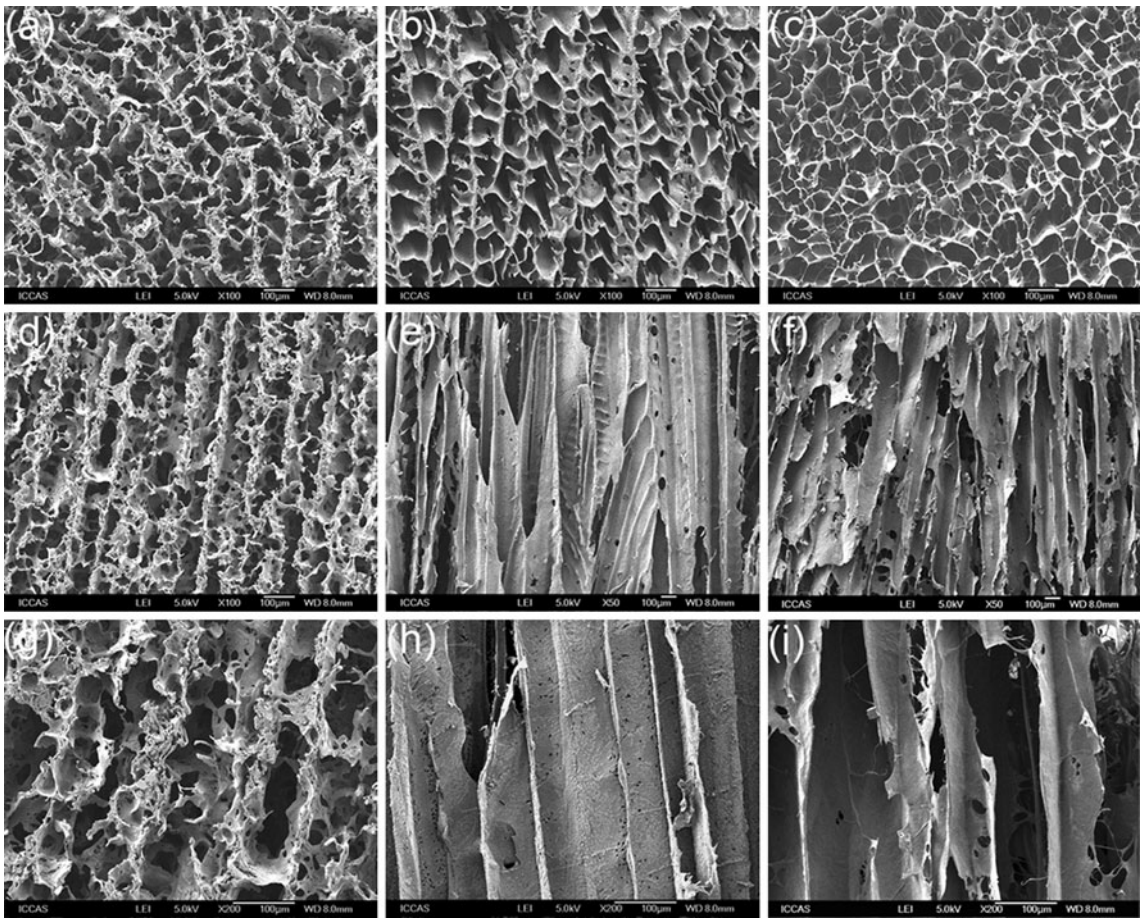

Fig. 3 SEM graphs of composite scaffold, PLGA and ACECM oriented scaffolds. View of the composite scaffold: **a**, **d**, **g**; view of the PLGA scaffold: **b**, **e**, **h**; view of the ACECM scaffold: **c**, **f**, **i**. cross section **a**, **b**, **c** and vertical section **d**–**i** of the oriented scaffolds respectively

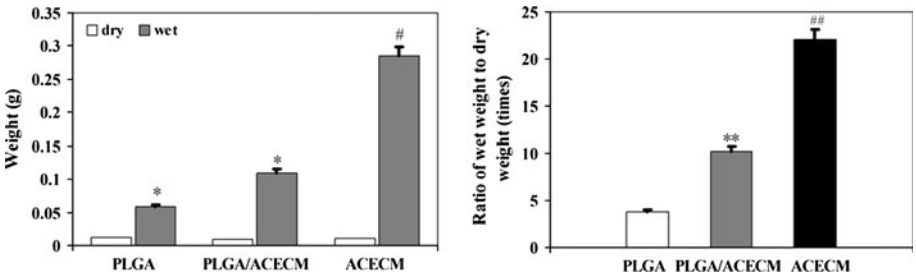

Fig. 4 Water uptake and ratio of wet weight to dry weight of PLGA, ACECM and composite scaffolds ($n = 9$). (*) $P < 0.05$ and ($^{\#}$) $P < 0.01$, wet weights comparison with dry weights of composite, PLGA and ACECM scaffold groups respectively. (**) $P < 0.05$ and ($^{\#\#}$) $P < 0.01$, in comparison with PLGA, composite scaffolds respectively of wet weight to dry weight

being cultured for 3 days. It could be seen that a few cells adhered on the wall of PLGA (Fig. 6a and d) scaffold. In the composite scaffold (Fig. 6b and e), three were many cells, which aligned along the vertical microtubules. The cells became well-rounded. In the ACECM scaffold (Fig. 6c and f), more cells showed a rounded morphology, good condition and aligned along vertical microtubules and run-through the scaffold.

3.6 Cell proliferation in oriented scaffolds

The proliferation of MSCs on three types of scaffolds was employed by the CCK-8 quantitative assay after cultured for 1, 3 and 7 days, as shown in Fig. 7. The MSCs in all the scaffolds were proliferating with time prolongation. The maximum and minimum of cells proliferation ability was observed on ACECM, PLGA scaffold respectively. At the

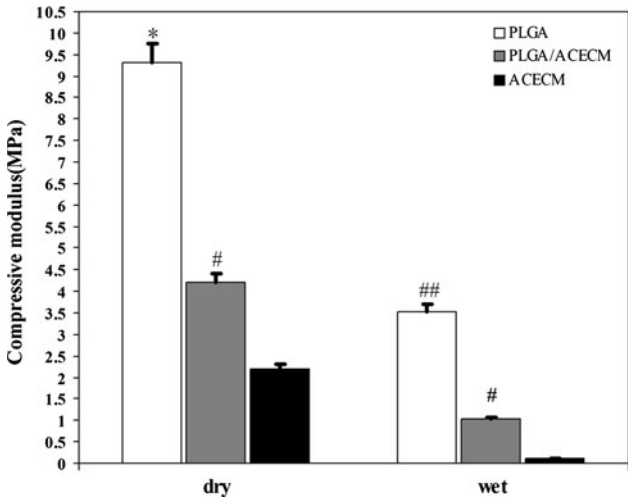

Fig. 5 Compressive modulus of PLGA, composite and ACECM scaffolds in dry and hydrous status. $n = 18$. (*) $P < 0.05$ and ($^{\#}$) $P < 0.01$, in comparison with composite, ACECM scaffolds groups respectively of dry status compressive modulus. ($^{\#\#}$) $P < 0.01$ and ($^{\#}$) $P < 0.01$, in comparison with composite, ACECM scaffolds group respectively of hydrous status compressive modulus

end of 7 days cells growth study, the OD value of CCK-8 was 2.535 ± 0.069 in ACECM scaffold, 2.204 ± 0.049 in composite scaffold, and 1.562 ± 0.198 in PLGA scaffold respectively. So the cells proliferation ability in ACECM or composite scaffolds was significantly higher than it was in the PLGA scaffold. The results were congruous with SEM graph and displayed that proliferated cells on composite scaffold was more than on PLGA scaffold.

3.7 Cell viability cultured on oriented scaffolds

The cell viability could be indicated in Fig. 8 after being seeded on three kinds of scaffolds on 3 and 7 days. On 3 days, there were some live cells (green spots) in PLGA (Fig. 8a) scaffold. Meanwhile, there were many green spots adhered on composite (Fig. 8b) and ACECM (Fig. 8c) scaffolds, in which cells aligned and distributed along the oriented microtubules. With the increasing of incubation time, more green spot could be observed and aligned along microtubules on 7 days (Fig. 8d, e and f). However, there were a few dead cells (red spots) dispersed sporadicly in the PLGA (Fig. 8g) scaffold; the dead cells were evidently few adhered on composite (Fig. 8h) and ACECM (Fig. 8i) scaffolds on incubation 7 days. The cells orientation distribution and viability were coincident with the results of SEM graphs and CCK-8 kit test.

4 Discussion

Tissue engineering scaffolds with biomimetic morphological structure and biochemical composition as that of ACECM were highly significant for facilitating cells adherence, proliferation and differentiation [28]. In this study, a composite oriented scaffold was fabricated by integrating nanofibrous ACECM with PLGA. This strategy pointed to that the scaffold should not only provide good cell affinity, strong mechanical strength but also possess biomimetic morphological structure to meet the requirements of cartilage structural regeneration.

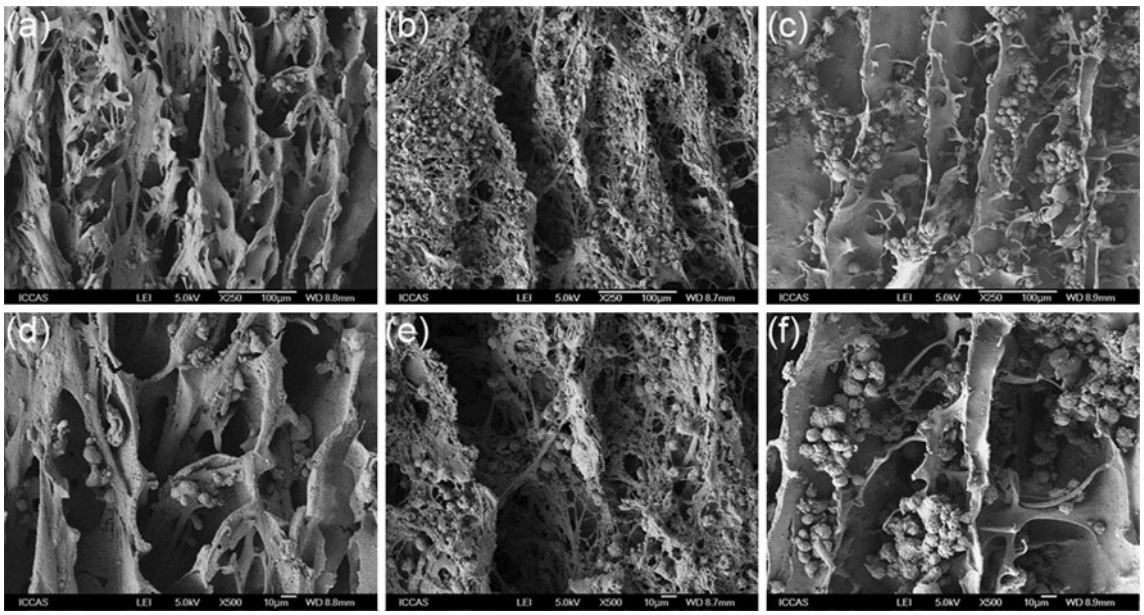

Fig. 6 SEM observation of MSCs cultured in the PLGA, composite and ACECM oriented scaffolds for 3 days. (PLGA scaffold: **a** and **d**; Composite scaffold: **b** and **e**; ACECM scaffold: **c** and **f**). **a**–**c**: magnification ×250; **d**–**f**: magnification ×500

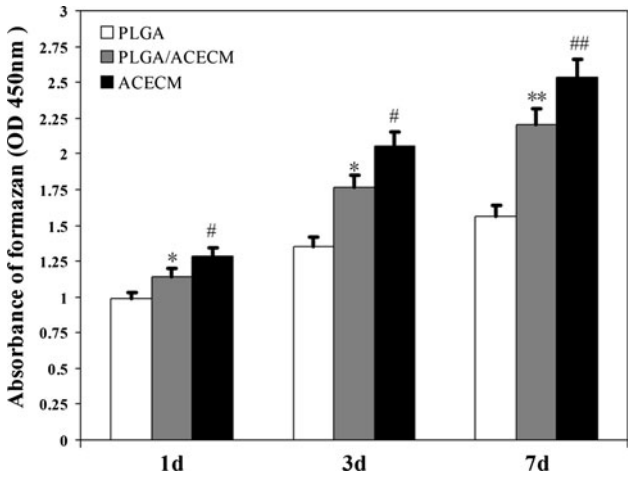

Fig. 7 CCK-8 assay cells proliferation of MSCs cultured in PLGA, composite and ACECM scaffolds in different culture days. $n = 12$. (*) $P < 0.05$ and ($^{\#}$) $P < 0.05$, in comparison with PLGA, composite scaffolds groups on 1 day and 3 days respectively. (**) $P < 0.01$ and ($^{\#\#}$) $P < 0.01$, in comparison with PLGA, composite scaffolds groups respectively on 7 days

The nanofibrous structure was advantageous for cells adherence, proliferation and tissue regeneration [29]. As one objective of this research was to fabricate nanofibrous ACECM oriented scaffold; however, it was significantly difficult to get acellular nanofibrous ACECM. Because cartilage was compact and hard, chondrocytes were encapsuled in cartilage surrounding ECM. In the procedure of decellularization, articular cartilage was difficult to be shattered and penetrated of solutions effectively. Cartilage particles under moist condition could absorb water sufficiently and become swell and soft. So, nanofibrous ACECM could be fabricated easily by pulverization in aqueous solution. With the differential centrifugation method, different size cartilage particles could be separated utmost. After decellularizing cells and digesting nuclear materials, acellular and nanofibrous cartilage ECM were collected ultimately. The results (Fig. 2) demonstrated that the ACECM was reserved remain after decellularization process and chemical cross linking.

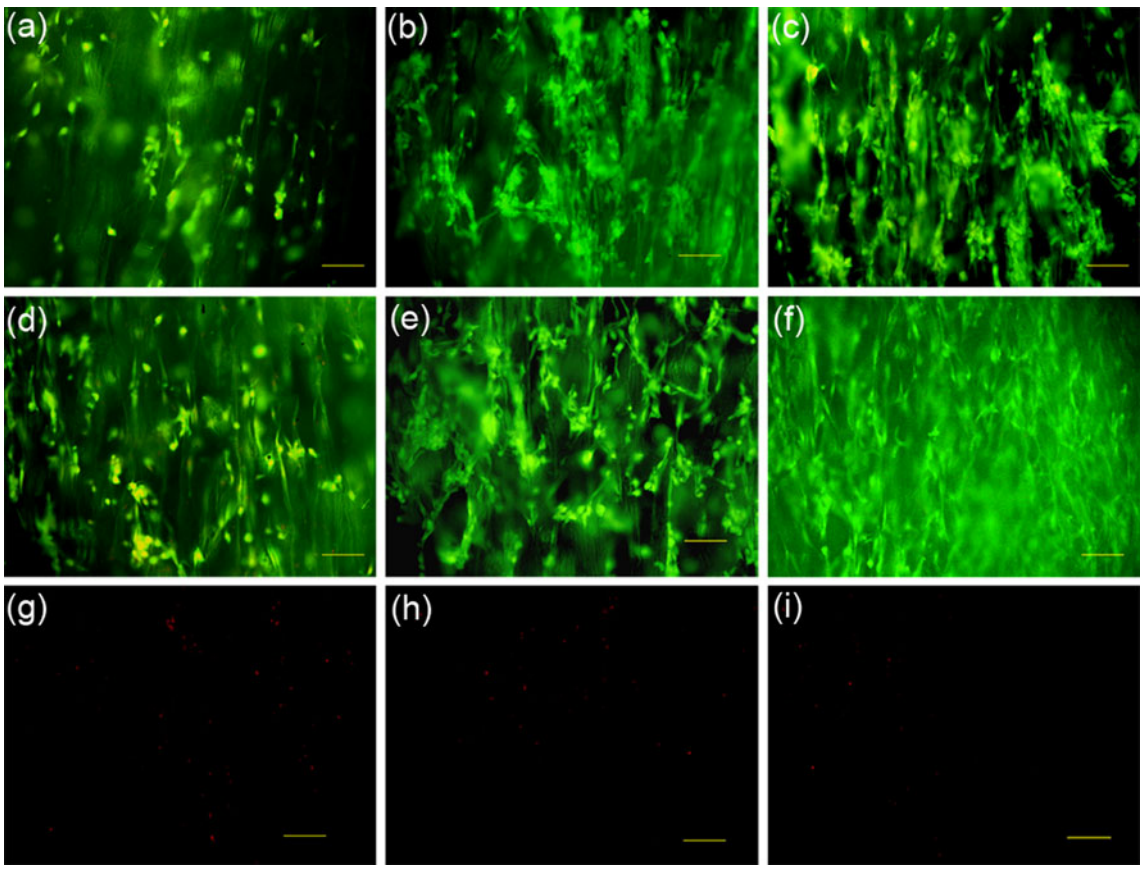

Fig. 8 Live/dead cells staining fluorescent photographs of MSCs cultured on oriented scaffolds. **a–c** cells cultured for 3 days; **d–i** cells cultured for 7 days. **a–f** live cells staining; **g–i** dead cells staining. **a**, **d**, **g** PLGA scaffold; **b**, **e**, **h** composite scaffold; **c**, **f**, **i** ACECM scaffold. *Bar* = 100 μm

According to the improved TIPS technique, the oriented PLGA scaffolds with varying pore diameter and porosity could be fabricated under suitable temperature gradient and cooling temperature [25]. As, in the existence of temperature gradient during phase separation, the fibrous crystals were produced by the crystal nucleus and then grew along orientation of temperature gradient. So the oriented scaffold with vertical microtubules could be fabricated after freeze drying. In this study, ACECM and PLGA/ACECM composite oriented scaffolds were fabricated by identical temperature gradient of the TIPS. So, the porosity and average pore diameter of three kinds of scaffolds were congruent almost and showed no statistical significance. The pore parameters including porosity and average pore diameter were extremely important for cells adherence and proliferation. Varying pore parameters could produce different results of cells proliferation and tissue regeneration [30]. So, it was eligible for the three types of oriented scaffolds with near equal pore parameters comparing with each other for their biological properties of mechanical strength, cells proliferation and viability.

The biomaterials with weak mechanical strength made it be difficult to withstand compression when implanted into the cartilage defect [18].The scaffolds with high mechanical strength not only play the role of temporary mechanical substitution, but also the stress stimulation can facilitate cells proliferation and differentiation. The persistent stress will promote the tissue engineering cartilage integration with surrounding junctional zone normal cartilage. In this study, the mechanical property of hydrous status was emphasized since cells-scaffolds structures were used in culture medium in vitro or exchanging fluid with synovia in vivo. The compressive modulus of hydrous ACECM scaffold was apparently low in contrast with dry status (Fig. 5). It was easily understood that the ACECM was hydrophilic, hydrous ACECM became soft and could not support strong compressive stress. After the ACECM combined with PLGA, the compressive modulus of hydrous composite scaffold was enhanced markedly. It was considered that PLGA have strong mechanical property than ACECM, meanwhile the water absorption of composite was reduced comparing with ACECM scaffold (Fig. 4). Therefore, the wall of composite scaffold was hard and could support powerful compressive stress than ACECM scaffold. Meanwhile, the oriented scaffolds possessed the anisotropic mechanical property which was biomimetic to the mechanical property of native cartilage [25]. According to the aforementioned results, it was concluded that the hydrous composite scaffold possesses more strong mechanical property than ACECM scaffold, which could support more powerful compressive stress than ACECM scaffold in vitro.

The SEM observation showed that MSCs adhered and aligned vertically along the microtubules of oriented scaffolds (Fig. 6). For tissue engineering applications, it was important to produce scaffolds with controlled orientation because alignment of the scaffolds predominantly guided cellular growth and spatial alignment [31]. In this research, the oriented scaffolds guided the MSCs growth and alignment. So, the MSCs adhered and aligned along the orientation of vertical microtubules, which was biomimetic to native physiological structure of deep zone cartilage. The cell affinity of scaffold was important for tissue regeneration and functional reconstruction. The CCK-8 quantitative test demonstrated that the cells adhered on oriented scaffolds were proliferating constantly with time prolongation (Fig. 7). The results of SEM observation and CCK-8 test manifested that the ACECM and composite scaffolds were more profit to cells adherence and proliferation than PLGA scaffold. As PLGA is a hydrophobic biomaterial. Usually, cells were difficult to migrate deeply into the PLGA scaffold for its hydrophobic surface. After the PLGA integrating with natural ACECM, which make the composite scaffold more hydrophilic apparently than PLGA scaffold (Fig. 4). Meanwhile, the ACECM with signal peptide was profit to cells adherence and proliferation. Otherwise, the pore diameter, porosity and pore structure of scaffolds were important for cells adherence and distribution [32, 33]. The oriented scaffold was convenient for cells adherence, migration into the inside of porous scaffold and nutrients exchanging. The micropores structure and rough surface of scaffold were also profit to cells adherence and migration [34, 35]. So, the high porosity, micropores and rough surface of oriented composite scaffold improved cells adherence and proliferation. So, the cell affinity of composite scaffold was improved markedly in contrast with PLGA scaffold.

Stem cells therapy possesses extensive perspective for tissue engineering application. So far, MSCs is the unique stem cell, which has been applied for cartilage restore in human body [36, 37]. After the MSCs being harvested and expanded in culture, which could be combined with a scaffold to repair cartilage defects. However, the development of scaffolds is a fundamental part for MSCs-based cartilage tissue engineering. In this study, the composite oriented scaffold was fabricated. The advantages included its bioactive ACECM and PLGA supported mechanical stress. The orientation of porous oriented scaffold was profit to seeding cells distribute to the interspace of scaffold and align along the vertical microtubules. The vertical microtubules were also beneficial to nutrients, bioactive macromolecule enter scaffold and metabolic waste discharge. The oriented composite scaffold possessed high porosity and microtubular wall with lots of micropores, which could load more cells. So, the oriented composite

scaffold with seeding cells was biomimetic to biomechanics and structural characteristics of deep zone cartilage. Future studies will investigate the application of this PLGA/ACECM composite scaffold loaded with MSCs to repair cartilage defects in animal models.

5 Conclusions

A biomimetic composite scaffold derived from natural nanofibrous ACECM and synthetic PLGA was fabricated by improved TIPS technique. The biomimetic scaffold possesses high porosity and well oriented microtubules structure. Comparing with oriented PLGA scaffold, the composite scaffold possesses preferable hydrophilicity and cell affinity for cells adhesion and proliferation. The composite scaffold possesses even higher mechanical strength than ACECM scaffold especially in the hydrous status. The oriented composite scaffold could guide cells alignment along the vertical orientation. The oriented structure was biomimetic to the deep zonal articular cartilage. It was demonstrated that the oriented composite scaffold was a potential candidate for application in cartilage tissue engineering.

Acknowledgments This study was funded by the National Natural Science Foundation of China (30973047, 2080409), National High-Tech Research and Development Program (2005CB522704, 2007 AA021902), National Science and Technology Supportive Program (2006BAI16B04).

References

1. Langer R, Vacanti JP. Tissue engineering. Science. 1993;260: 920–6.
2. Nerem RM, Sambanis A. Tissue engineering: from biology to biological substitutes. Tissue Eng. 1995;1:3–13.
3. Jeong SI, Kim SY, Cho SK, Chong MS, Kim KS, Kim H, et al. Tissue-engineered vascular grafts composed of marine collagen and PLGA fibers using pulsatile perfusion bioreactors. Biomaterials. 2007;28:1115–22.
4. Hui TY, Cheung KMC, Cheung WL, Chan D, Chan BP. In vitro chondrogenic differentiation of human mesenchymal stem cells in collagen microspheres: influence of cell seeding density and collagen concentration. Biomaterials. 2008;29:3201–12.
5. Yamane S, Iwasaki N, Majima T, Funakoshi T, Masuko T, Harada K, et al. Feasibility of chitosan-based hyaluronic acid hybrid biomaterial for a novel scaffold in cartilage tissue engineering. Biomaterials. 2005;26:611–9.
6. Zhang L, Ao Q, Wang AJ, Lu GY, Kong LJ, Gong YD, et al. A sandwich tubular scaffold derived from chitosan for blood vessel tissue engineering. J Biomed Mater Res Part A. 2006;77A: 277–84.
7. Wang Y, Bella E, Lee CS, Migliaresi C, Pelcastre L, Schwartz Z, et al. The synergistic effects of 3-D porous silk fibroin matrix scaffold properties and hydrodynamic environment in cartilage tissue regeneration. Biomaterials. 2010;31:4672–81.
8. Hu J, Feng K, Liu XH, Ma PX. Chondrogenic and osteogenic differentiations of human bone marrow-derived mesenchymal stem cells on a nanofibrous scaffold with designed pore network. Biomaterials. 2009;30:5061–7.
9. Jung Y, Park MS, Lee JW, Kim YH, Kim SH, Kim SH. Cartilage regeneration with highly-elastic three-dimensional scaffolds prepared from biodegradable poly (L-lactide -co-3-caprolactone). Biomaterials. 2008;29:4630–6.
10. Uematsu K, Hattori K, Ishimoto Y, Yamauchi J, Habata T, Takakura Y, et al. Cartilage regeneration using mesenchymal stem cells and a three-dimensional poly lactic-glycolic acid (PLGA) scaffold. Biomaterials. 2005;26:4273–9.
11. Wen XJ, Tresco PA. Fabrication and characterization of permeable degradable poly(D, L-lactide-co-glycolide) (PLGA) hollow fiber phase inversion membranes for use as nerve tract guidance channels. Biomaterials. 2006;27:3800–9.
12. Richard RD, Aldor RB, Veronique M, Sandra S, Alastair F, Simon G, et al. In vivo characterization of a novel bioresorbable poly(lactide-co-glycolide) tubular foam scaffold for tissue engineering applications. J Mater Sci Mater Med. 2004;15:729–34.
13. Liu Y, Bharadwaj S, Lee SJ, Atala A, Zhang YY. Optimization of a natural collagen scaffold to aid cell–matrix penetration for urologic tissue engineering. Biomaterials. 2009;30:3865–73.
14. Zhao YL, Zhang S, Zhou JY, Wang JL, Zhen MC, Liu Y, et al. The development of a tissue-engineered artery using decellularized scaffold and autologous ovine mesenchymal stem cells. Biomaterials. 2010;31:296–307.
15. Zhang XJ, Deng ZH, Wang HL, Yang ZH, Guo WH, Li Y, et al. Expansion and delivery of human fibroblasts on micronized acellular dermal matrix for skin regeneration. Biomaterials. 2009;30:2666–74.
16. Yang Q, Peng J, Guo QY, Huang JX, Zhang L, Yao J, et al. A cartilage ECM-derived 3-D porous acellular matrix scaffold for in vivo cartilage tissue engineering with PKH26-labeled chondrogenic bone marrow-derived mesenchymal stem cells. Biomaterials. 2008;29:2378–87.
17. Gratz KR, Wong VW, Chen AC, Fortier LA, Nixon AJ, Sah RL. Biomechanical assessment of tissue retrieved after in vivo cartilage defect repair: tensile modulus of repair tissue and integration with host cartilage. J Biomech. 2006;36:138–46.
18. Gotterbarm T, Richter W, Jung M, Berardi Vilei S, Mainil-Varlet P, Yamashita T, et al. An in vivo study of a growth-factor enhanced, cell free, two-layered collagen–tricalcium phosphate in deep osteochondral defects. Biomaterials. 2006;27:3387–95.
19. Lanfer B, Seib FP, Freudenberg U, Stamov D, Bley T, Bornhäuser M, et al. The growth and differentiation of mesenchymal stem and progenitor cells cultured on aligned collagen matrices. Biomaterials. 2009;30:5950–8.
20. Lanfer B, Hermann A, Kirsch M, Freudenberg U, Reuner U, Werner C, et al. Directed growth of adult human white matter stem cell-derived neurons on aligned fibrillar collagen. Tissue Eng Part A. 2010;16:1103–13.
21. Tan HP, Wu JD, Lao LH, Gao CY. Gelatin/chitosan/hyaluronan scaffold integrated with PLGA microspheres for cartilage tissue engineering. Acta Biomater. 2009;5:328–37.
22. Dai WD, Kawazoe N, Lin XT, Dong J, Chen GP. The influence of structural design of PLGA/collagen hybrid scaffolds in cartilage tissue engineering. Biomaterials. 2009;30:1–12.
23. Wu SC, Chang JK, Wang CK, Wang GJ, Ho ML. Enhancement of chondrogenesis of human adipose derived stem cells in a hyaluronan-enriched microenvironment. Biomaterials. 2010;31:631–40.
24. Shi GX, Cai Q, Wang CY, Lu N, Wang SG, Bei JZ. Fabrication of cell scaffold of poly(L-lactic acid) and poly(L-lactic-co-glycolic acid) and biocompatibility. Polym Adv Technol. 2002; 13:227–32.

25. Yang F, Qu X, Cui WJ, Bei JZ, Yu FY, Lu SB, et al. Manufacturing and morphology structure of polylactide-type microtubules orientation structured scaffolds. Biomaterials. 2006;27:4923–33.
26. Ma PX, Zhang RY. Microtubular architecture of biodegradable polymer scaffolds. J Biomed Mater Res. 2001;56:469–77.
27. Yang HN, Park JS, Na K, Woo DG, Kwon YD, Park KH. The use of green fluorescence gene (GFP)-modified rabbit mesenchymal stem cells (rMSCs) co-cultured with chondrocytes in hydrogel constructs to reveal the chondrogenesis of MSCs. Biomaterials. 2009;30:6374–85.
28. Wise JK, Yarin AL, Megaridis CM, Cho M. Chondrogenic differentiation of human mesenchymal stem cells on oriented nanofibrous scaffolds: engineering the superficial zone of articular cartilage. Tissue Eng Part A. 2009;15:913–21.
29. Li WJ, Jiang YJ, Tuan RS. Chondrocyte phenotype in engineered fibrous matrix is regulated by fiber size. Tissue Eng. 2006;12:1775–85.
30. Roosa SM, Kemppainen JM, Moffitt EN, Krebsbach PH, Hollister SJ. The pore size of polycaprolactone scaffolds has limited influence on bone regeneration in an in vivo model. J Biomed Mater Res A. 2010;92:359–68.
31. Yang F, Murugan R, Wang S, Ramakrishna S. Electrospinning of nano/micro scale poly (L-lactic acid) aligned fibers and their potential in neural tissue engineering. Biomaterials. 2005;26:2603–10.
32. Lee M, Wu BM, Dunn JC. Effect of scaffold architecture and pore size on smooth muscle cell growth. J Biomed Mater Res A. 2008;87:1010–6.
33. Kasten P, Beyen I, Niemeyer P, Luginbuhl R, Bohner M, Richter W. Porosity and pore size of beta-tricalcium phosphate scaffold can influence protein production and osteogenic differentiation of human mesenchymal stem cells: an in vitro and in vivo study. Acta Biomater. 2008;4:1904–15.
34. Campbell CE, von Recum AF. Microtopography and soft tissue response. J Invest Surg. 1989;2:51–74.
35. Deligianni DD, Katsala ND, Koutsoukos PG. Effect of surface roughness of hydroxyapatite on human bone marrow cell adhesion, proliferation, differentiation and detachment strength. Biomaterials. 2001;22:87–96.
36. Kuroda R, Isada K, Matsumoto T, Akisue T, Fujioka H, Mizuno K, et al. Treatment of a full-thickness articular cartilage defect in the femoral condyle of an athlete with autologous bone-marrow stromal cells. Osteoarthr Cartil. 2007;15:226–31.
37. Wakitani S, Imoto K, Yamamoto T, Saito M, Murata N, Yoneda M, et al. Human autologous culture expanded bone marrow mesenchymal cell transplantation for repair of cartilage defects in osteoarthritis knees. Osteoarthr Cartil. 2002;10:199–206.